PROCEEDINGS OF SCIENCE

Effects of inhomogeneous stellar winds in the emission of gamma-ray binaries

Elina Kefala^{1,2,3,*} **and Valentí Bosch-Ramon**^{1,2,3}

[1] *Departament de Física Quàntica i Astrofísica (FQA), Universitat de Barcelona (UB),*
Martí i Franqués, 1, 08028 Barcelona, Spain

[2] *Institut de Ciències del Cosmos (ICCUB), Universitat de Barcelona (UB),*
Martí i Franqués, 1, 08028 Barcelona, Spain

[3] *Institut d'Estudis Espacials de Catalunya (IEEC),*
Gran Capità, 2-4, 08034 Barcelona, Spain

E-mail: `ekefala@icc.ub.edu`, `vbosch@fqa.ub.edu`

We study the interaction between a pulsar and an inhomogeneous stellar wind in gamma-ray binaries. In such systems, the acceleration of particles likely occurs at the region of collision between the two winds, which is typically assumed to be smooth. However, the early-type stars that are thought to be present in some gamma-ray binaries appear to have clumpy winds. During the two-wind interaction, these clumps arrive at the acceleration region, reshape the interaction structure, and subsequently impact the related non-thermal emission. Depending on the adopted stellar wind parameters, the clumps can produce observable fluctuations in the X-ray and gamma-ray bands. Semi-analytical calculations of the dynamical evolution and the non-thermal emission allow the study of clump-induced small-scale variability of such systems.

7th Heidelberg International Symposium on High-Energy Gamma-Ray Astronomy (Gamma2022)
4-8 July 2022
Barcelona, Spain

PoS(Gamma2022)150

---

[*] Speaker

1. Physical scenario

In a high-mass gamma-ray binary harboring a young pulsar, the contact discontinuity (CD) formed by the collision of the stellar and pulsar winds can be reshaped by wind inhomogeneities (clumps) of the high-mass star interacting with the pulsar wind. Single interactions have been studied elsewhere with relativistic hydrodynamic simulations [1] to compute the non-thermal emission [2], but full hydrodynamic codes are very computationally demanding to model the collective effect of multiple events. In this work, stellar wind inhomogeneity is introduced in the form of spherical clumps generated by a Monte Carlo simulation that determines their size/mass, and time and direction of launch from the stellar surface. Then, semi-analytical calculations are used to compute the dynamics of the clumps and the related emission.

For the simulation, a system with properties similar to those of LS 5039 [3] was considered. The massive star has a luminosity of $L_* = 10^{39}$ erg s^{-1} and a temperature of $T_* = 4 \times 10^4$ K, which yield a radius of $R_* = 10.5\,\mathrm{R}_\odot$. The stellar wind is considered to be supersonic, with a constant velocity of $u_\mathrm{w} = 2 \times 10^8$ cm s^{-1}, and has a mass-loss rate of $\dot{M} = 10^{-7}\,\mathrm{M}_\odot$ yr^{-1}. The clumpy component of the stellar wind is described by a top-heavy mass distribution $\propto M_\mathrm{c}^{-2}$, where M_c is the clump mass, and a volume filling factor $f = 0.1$. A non-accreting pulsar moves around the massive star in an elliptical orbit with eccentricity $e = 0.35$, semi-major axis $\alpha = 2.1 \times 10^{12}$ cm, and periodicity $P = 3.91$ days. The pulsar powers an isotropic relativistic wind with bulk Lorentz factor $\Gamma_\mathrm{w} = 10^5$ and power $P_\mathrm{sd} = 3 \times 10^{36}$ erg s^{-1}. The system is taken to be at 3 kpc from the Earth.

2. CD Distortion by Clumps

The shape of the initially smooth CD is found by equating the wind ram pressures [4] and tilting the entire structure by an angle to account for orbital Coriolis effects. This shape is deformed by the interaction of the pulsar wind with clumps arriving at the region. Large enough clumps will penetrate the pulsar wind termination shock [5], expand at the shocked-clump sound speed under the impact of the pulsar wind ram pressure, and cause large and rapid distortions of the CD structure. Beyond the CD, the dynamic evolution of the clumps shocked by a relativistic flow is described by a semi-analytical hydrodynamical model presented in the appendix of Barkov et al. [6], plus Coriolis deflection.

Figure 1 gives an idea of the extent of distortion of the CD, including regions up to a distance 1.5 times the orbital separation d at an intermediate orbital phase (at which the line of sight is perpendicular to the pulsar–emitter line). The CD structure largely diverges from the smooth-wind case and is quickly deformed as clumps penetrate the two-wind region and then get deflected, dissolve, and mix with the shocked material. Details on the derivation of the clump trajectories and dynamics, as well as results for stellar wind scenarios with different degrees of inhomogeneity, can be found in [7].

3. Clump Effect on Emission

Large divergences of the CD structure from the smooth-wind CD result in changes in the emitter properties and thus observable changes in the produced spectral energy distributions (SEDs). Here,

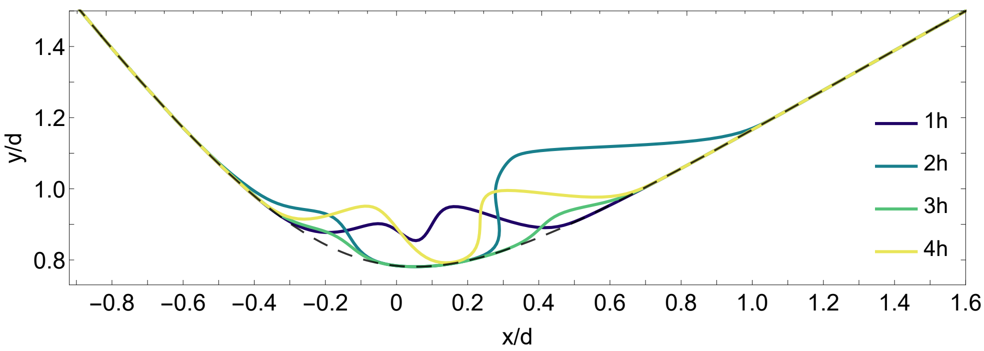

Figure 1: 2D snapshots of the CD at 1 hour intervals (solid lines) and for a smooth stellar wind (dashed line). The simulated region extends up to $1.5d$ from the star at an intermediate orbital phase.

the disturbed CD is treated as a multi-zone emitting region, and the non-thermal emission is modeled considering only electrons/positrons that cool by synchrotron and inverse Compton (IC) in two extreme cooling regimes, the saturation and adiabatic regimes. In the saturation regime, the energy distribution of rapidly cooling particles is directly determined by radiative losses and the injected energy distribution. Here, we take an injection power law of index 2 with an exponential cut-off, with a minimum particle energy of 100 MeV and a maximum electron energy determined by acceleration, radiative losses, and escape. When escape dominates, it is the total energy density stored in the shock region that determines the normalization of the particle distribution (adiabatic regime), and the power-law index is still 2.

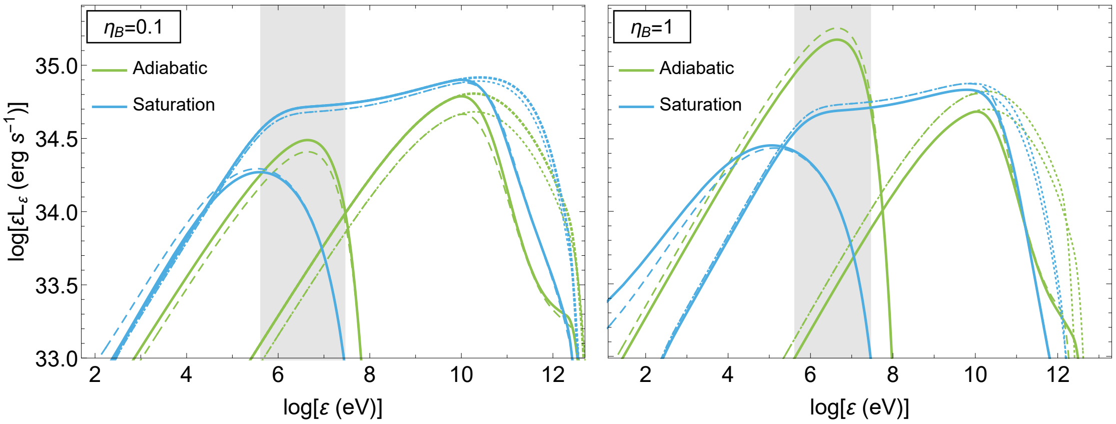

(a) (b)

Figure 2: X-ray to TeV SEDs for the smooth stellar wind case (dashed lines) and the clumpy snapshot at 2 hours shown in Fig. 1 (solid lines) for the two regimes for two η_B values. The unabsorbed spectra are marked by dotted lines. Both the adiabatic (green lines) and saturation (blue lines) regimes are shown. The shaded area marks the transition from the adiabatic to the radiative regime for IC scattering. The transition region for synchrotron occurs at lower energies ($\sim 10^{-2}$ eV) not shown in the plot.

In Fig. 2, we compare the SEDs for the smooth and distorted CDs for two values of the magnetic-to-plasma energy density ratio η_B (which corresponds to magnetic-to-stellar photon energy density ratios of $\eta_* = 10^{-2}\eta_B$). Larger changes are observed in the adiabatic regime, which is directly affected by changes in the size (thickness) of the emitting region besides changes in the magnetic and photon fields. However, we expect the radiative regime to be more realistic overall. For a moderate η_B value (left), X-rays and gamma rays are dominated by IC losses. Only for a strongly magnetized pulsar wind (right), X-rays are characterized by synchrotron emission.

4. Clump-induced Variability

Stellar wind clumps can be an origin of short-scale variability in gamma-ray binaries, as captured by the light curves in Fig. 3, which exhibit some fluctuations in the flux of approximately 10–20%. The flux basically scales linearly with the inclination toward the line-of-sight direction. Fluctuations in the adiabatic regime are mainly associated with reductions and increments in the total emitting volume. Therefore, this regime generally better captures the primary geometric effects, especially those related to emission from the outer parts of the CD. Fluctuations in the fully radiative regime mostly originate from enhancements in the magnetic field due to local changes in the emitter–pulsar distance and IC and gamma-ray absorption angular effects in the high energies (HE; 0.1–10 GeV) and very high energies (VHE; > 100 GeV). The enhancement in the synchrotron versus IC emissivity results in a peak of approximately a factor of 2 above the baseline flux in the X-rays in the saturation regime.

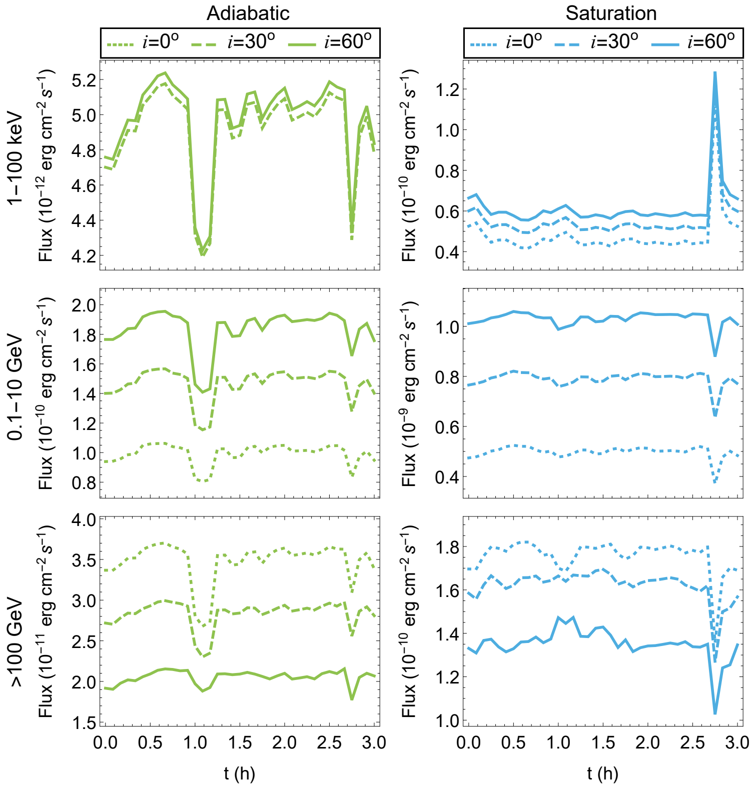

Figure 3: Light curves over a period of 3 hours for different inclinations $i = 0°$ (dotted lines), 30° (dashed lines), and 60° (solid lines). The energy bands shown are X-rays (1–100 keV, synchrotron only; top rows), HE (0.1–10 GeV, IC only; middle rows), and VHE gamma rays (> 100 GeV, IC only; bottom rows) for $\eta_B = 0.1$. Both the adiabatic (green lines; left column) and saturation (blue lines; right column) regimes are shown.

We note that the light curves are computed considering only synchrotron losses in the X-rays and only IC losses in the HE and VHE bands as these are typically the dominant cooling processes in these bands in the cases studied (although in the saturation, weakly magnetized case, the synchrotron and IC losses are comparable in the X-rays; see Fig. 2a). This still provides accurate enough results for our purposes and allows for a more intuitive understanding of the emission behavior. A more extensive study of such a physical scenario and a discussion on how certain parameters (e.g., the clump mass distribution and filling factor, the emitter size, and the wind momentum rate ratio) can affect the frequency of interactions and the induced variability is provided in [7].

5. Discussion

Clumpy stellar winds may introduce fluctuations in the luminosity, with relative flux changes of 10–20%, mainly originating in the lower-energy adiabatic regions of the particle distribution, and even up to 100% in events involving very large clumps in a fully radiative regime. Therefore, the effect of clumps should not be entirely overlooked as interactions of the shocked pulsar wind with large clumps can still occur from time to time. Although infrequent, such interactions can significantly perturb the emitting region leading to observable flux variations. Our simple semi-analytical approach allows us to quickly but robustly estimate the effects of stellar winds with different degrees of inhomogeneity and model the highly diverse population of gamma-ray binaries. Application of our model is limited though to regions close to the pulsar where the shocked flow is still subsonic. Beyond this region, a more complex model is necessary to account for the complicated hydrodynamics and orbital effects.

Acknowledgments

The authors acknowledge financial support from the State Agency for Research of the Spanish Ministry of Science and Innovation under grant PID2019-105510GB-C31 and through the ”Unit of Excellence María de Maeztu 2020-2023” award to the Institute of Cosmos Sciences (CEX2019-000918-M). V.B-R. is a Correspondent Researcher of CONICET, Argentina, at the IAR.

References

[1] X. Paredes-Fortuny, V. Bosch-Ramon, M. Perucho and M. Ribó, *Simulations of an inhomogeneous stellar wind interacting with a pulsar wind in a binary system*, *A&A* **574** (2015) A77 [`1411.3593`].

[2] V.M. de la Cita, S. del Palacio, V. Bosch-Ramon, X. Paredes-Fortuny, G.E. Romero and D. Khangulyan, *Gamma rays from clumpy wind-jet interactions in high-mass microquasars*, *Astronomy & Astrophysics* **604** (2017) A39.

[3] J. Casares, M. Ribó, I. Ribas, J.M. Paredes, J. Martí and A. Herrero, *A possible black hole in the γ-ray microquasar LS 5039*, *MNRAS* **364** (2005) 899 [`astro-ph/0507549`].

[4] J. Cantó, A.C. Raga and F.P. Wilkin, *Exact, Algebraic Solutions of the Thin-Shell Two-Wind Interaction Problem*, *ApJ* **469** (1996) 729.

[5] V. Bosch-Ramon, *Clumpy stellar winds and high-energy emission in high-mass binaries hosting a young pulsar*, *A&A* **560** (2013) A32 [`1310.5641`].

[6] M.V. Barkov, F.A. Aharonian, S.V. Bogovalov, S.R. Kelner and D. Khangulyan, *Rapid TeV Variability in Blazars as a Result of Jet-Star Interaction*, *ApJ* **749** (2012) 119 [`1012.1787`].

[7] E. Kefala and V. Bosch-Ramon, *Modeling the effects of clumpy winds in the high-energy light curves of γ-ray binaries*, *A&A* (2022) [in press].